J Mater Sci (2011) 46:6744–6750
DOI 10.1007/s10853-011-5630-5

Synthesis and morphology of new functional polyimide/titania nano hybrid materials

Hojjat Seyedjamali · Azadeh Pirisedigh

Received: 31 December 2010 / Accepted: 21 February 2011 / Published online: 20 May 2011

Abstract The synthesis and full characterization of 3, 5-diamino-*N*-(1-oxo-3-phenyl-1-(phenylamino)propan-2-yl)benzamide (**5**), as a new diamine monomer containing L-phenylalanine fractions in the structure of pendant group is presented. The stated diamine is employed as a key monomer for the in situ sol–gel fabrication of polyimide/titania nano hybrid thin films containing different titania contents. It is shown that titania particles are created in the size range of 20–80 nm, well-dispersed and enjoy the favorable spherical shapes supposing the constructive organic–inorganic interactions. The superior thermal stabilities of resulted nanocomposite films are confirmed using thermal analysis techniques. Moreover, the UV–Vis spectroscopy has shown the growing up in blocking efficiency along with the increase in titania contents. Predictably, the produced titania nanoparticles have amorphous structures.

Introduction

In recent years, fabrication of organic–inorganic nanocomposite (NC) materials remains an attractive field of investigations due to the new and versatile characteristics of these innovative nano hybrid materials [1–8]. The superior thermal, optical, and mechanical properties are some of the advantages of well-dispersed NCs over the traditional macroscale hybrid materials [5–8].

Among the inorganic nanoparticles, TiO_2 (titania) possess an exclusive situation due to the widespread motivating properties such as high refractive index, photocatalytic activity, low birefringence, and of course low cost [1–7]. Recently, several efforts have been aimed at the production of titania NCs for the use as gas separation membranes [9], optical devises [10], fuel cells [11], catalysts for organic pollutant photodegradation [12, 13], etc.

The adjustment of organic/inorganic phases controls the nano-dimensional properties of nano hybrid materials mainly because of its effect on the nanoparticles distributions [14, 15]. In general, the organic/inorganic adjustment achieves via either the construction of chemical bonds or physical attractions between these intrinsically different phases [16, 17]. In the chemical modifications, suitable linkers graft to organic grounds and/or inorganic phases covalently [18, 19]. Thus, this technique may disturb the desired properties of final products, besides the increasing of the synthesis steps as well as the production costs. On the contrary, in the physical adjustment mode, the formation of organic/inorganic interactions such as H-bonds is operated. In fact, the polymer backbone acts as an internal dispersant agent. The physical adaptation is preferred principally due to the more simplicity and dispensable preconditions [17]. The in situ sol–gel creation of inorganic nanoparticles within the polymer matrixes is one of the most important methodologies to fabricate the well-dispersed nano hybrid materials by means of physical organic/inorganic interactions [20, 21].

Polyimides (PIs) are the imperative engineering macromolecules and promising NC matrixes due to the several interesting characteristics such as superior stabilities toward chemicals and elevated temperatures, low thermal expansion coefficient, and high mechanical strength [21–25]. PIs may be simply synthesized via the polycondensation of diamines and dianhydrides. Interestingly, the sol–gel procedure shows an excellent conformity with the

H. Seyedjamali (✉) · A. Pirisedigh
Department of Chemistry, Islamic Azad University, Kazerun Branch, Kazerun, Iran
e-mail: seyedjamali@yahoo.com; hojjat.seyedjamali@kau.ac.ir

stepwise PIs synthesis [22]. Although PIs suffer the low processability which may diminishes their applications, but it may be improved through several conventional techniques such as incorporation of unsymmetrical, bulky or flexible substitutions into the polymer chains as well as pendant groups [23–25].

On the other hand, the synthesis and application of advanced materials containing natural species have attracted great recent attentions mainly due to the interesting biological and/or chiroptical properties [26–28]. Naturally accruing α-amino acids have been widely used in the main chains of biopolymers as well as pendant groups [29–31]. The term bio-nanocomposite refers to the expansion of this contemporary part of science to the nano hybrid materials [32–34]. We have recently reported the sol–gel fabrication of a series of nano hybrid thin films containing L-leucine moieties in the polymer main chains [35]. Herein, we wish to report the in situ sol–gel fabrication of a series of well-dispersed PI/titania nano hybrid films containing L-phenylalanine in the structure of polymer matrixes as a fraction of pendant groups. Of course, the study of potential bioactivity of the fabricated NCs is not the subject of current report.

Experimental

Materials

All chemicals were purchased from Fluka Chemical Co. (Buchs, Switzerland), Aldrich Chemical Co. (Milwaukee, WI), Riedel-de Haen AG (Seelze, Germany), and Merck Chemical Co. Pyromellitic dianhydride (PMDA) was recrystallized from acetic anhydride and then dried in a vacuum oven at 120 °C overnight. *N,N*-dimethylformamide (DMF) was dried over barium oxide, followed by fractional distillation. L-phenylalanine methyl ester hydrochloride, hydrazine monohydrated, Tetraethyl orthotitanate ($Ti(OEt)_4$), and acetylacetone (acac) were employed as received.

Measurements

Proton nuclear magnetic resonance (^{1}H NMR, 500 MHz and ^{13}C-NMR, 125 MHz) spectra were recorded in DMSO-d_6 solution using a Bruker (Germany) Avance 500 instrument. Proton resonances are designated as singlet (s), doublet (d), quartet (q), and multiplet (m). FT–IR spectra were recorded on 400D IR spectrophotometer (Japan). The vibrational transition frequencies are reported in wave numbers (cm^{-1}). Band intensities are assigned as weak (w), medium (m), strong (s), and broad (br). Thermal gravimetric analysis (TGA) data were taken on Perkin Elmer in nitrogen atmosphere at a heating rate of 20 °C min^{-1}. Differential scanning calorimetry (DSC) data were recorded on a DSC-PL-1200 instrument at a heating rate of 20 °C min^{-1} in nitrogen atmosphere. The X-ray diffraction (XRD) patterns were recorded by employing a Philips X'PERT MPD diffractometer (Cu Kα radiation: $\lambda = 0.154056$ nm at 40 kV and 30 mA) over the 2θ range of 20–80° at a scan rate of 0.05° min^{-1}. Transmission electron microscopy (TEM) images were recorded using a JEOL JEM-2000. UV–Visible absorbance spectra were obtained from Perkin UV–VIS lambda 850 spectrometer.

Synthesis of methyl 2-(3,5-dinitrobenzamido)-3-phenylpropanoate (**3**)

A solution of L-phenylalanine methyl ester hydrochloride (**1**) (5.00 g, 23 mmol); triethylamine (1.5 mL); and 3,5-dinitrobenzoyl chloride (**2**) (5.35 g, 23 mmol) in $CHCl_3$ (50 mL) was stirred at room temperature. The end of reaction was controlled by TLC (50:50 ethylacetate: *n*-hexane). The reaction mixture was washed with water (75 mL × 3) and then, the organic layer was separated and dried over calcium chloride and concentrated by rotary evaporation. The residue was purified by recrystallization from ethylacetate/*n*-hexane and vacuum dried to yield, 8.07 g (94%) of dinitro compound 3 as a white precipitate; $[\alpha]_D^{25} = -19.7°$ cm^3 g^{-1} dm^{-1} ($c = 0.005$ g cm^{-3} in DMF). FT–IR (KBr): 3330 (m), 3077 (m), 1733 (s), 1654 (s), 1620 (m), 1630 (m), 1533 (s), 1465 (m), 1342 (s), 1283 (s), 1200 (m), 1151 (m), 711 (s) cm^{-1}. ^{1}H-NMR (500 MHz, DMSO, d_6): δ 3.05–3.28 (dd, $J_1 = 13.88$, $J_2 = 7.54$, 2H), 3.78 (s, 3H), 4.72 (dd, $J_1 = 7.63$, $J_2 = 6.12$, 1H), 7.25(Ar–H, 1H), 7.31 (Ar–H, 2H), 7.43 (Ar–H, 2H), 9.05 (Ar–H, 1H), 9.13 (Ar–H, 2H), 9.7 (amide N–H, 1H) ppm. ^{13}C-NMR (125 MHz, DMSO, d_6): δ 37.28 (CH_2), 53.12 (CH_3), 54.35 (CH), 121.35 (Ar), 126.43 (Ar), 128.05 (Ar), 129.11 (Ar), 129.75 (Ar), 136.19 (Ar), 137.24 (Ar), 150.39 (Ar), 168.56 (C=O), 172.81 (C=O) ppm. Elemental analysis calculated for $C_{17}H_{15}N_3O_7$ (373.32 g mol^{-1}): C, 54.69%; H, 4.05%; N, 11.26%. Found: C, 54.15%; H, 4.27%; N, 10.83%.

Synthesis of 3,5-dinitro-*N*-(1-oxo-3-phenyl-1-(phenylamino)propan-2-yl)benzamide (**4**)

A solution of dinitro compound **3** (5.3 g, 13 mmol) and 1.3 mL of distilled aniline in 10 mL of DMF was prepared and refluxed over night. Then DMF was evaporated under reduced pressure and the reaction mixture was poured into a mixture of 100 mL of distilled water and 2 mL of concentrated HCl. Compound **4** as a white precipitate was formed which was filtered off, washed with distilled water and vacuum dried. The yield was 91% (5.6 g);

$[\alpha]_D^{25} = -12.02°$ cm^3 g^{-1} dm^{-1} ($c = 0.005$ g cm^{-3} in DMF). FT–IR (KBr): 3335 (m), 3072 (m), 1690 (s), 1689 (s), 1623 (m), 1645 (m), 1522 (s), 1412 (m), 1327 (s), 1207 (s), 1189 (m), 1150 (m) cm^{-1}. ^{1}H-NMR (500 MHz, DMSO, d_6): 3.57 (dd, $J_1 = 14.03$, $J_2 = 7.92$, 2H), 4.85 (dd, $J_1 = 7.65$, $J_2 = 6.37$, 1H), 7.23 (Ar–H, 1H), 7.35 (Ar–H, 1H), 7.38 (Ar–H, 2H), 7.40 (Ar–H, 4H), 7.63 (Ar–H, 2H), 8.92 (amide N–H, 1H), 9.06 (Ar–H, 1H), 9.14 (Ar–H, 2H), 9.73 (amide N–H, 1H) ppm. ^{13}C-NMR (125 MHz, DMSO, d_6): δ 37.25 (CH2), 53.15 (CH), 121.33 (Ar), 122.43 (Ar), 126.39 (Ar), 128.07 (Ar), 128.50 (Ar), 129.77 (Ar), 129.12 (Ar), 129.78 (Ar), 136.21 (Ar), 137.25 (Ar), 139.11 (Ar), 150.37 (Ar), 168.51 (C=O), 172.82 (C=O) ppm. Elemental analysis calculated for $C_{22}H_{18}N_4O_6$ (434.40 g mol^{-1}): C, 60.83%; H, 4.18%; N, 12.90%. Found: C, 60.64%; H, 4.35%; N, 12.71%.

Synthesis of 3,5-diamino-*N*-(1-oxo-3-phenyl-1-(phenylamino)propan-2-yl)benzamide (**5**)

In a 100 mL two necked round-bottomed flask equipped with a reflux condenser and a dropping funnel, a suspension of compound **4** (5.0 g, 11.5 mmol), Pd–C 10% (0.4 g) and DMF (20 mL) was prepared. The mixture was warmed and at the same time as being stirred magnetically, hydrazine monohydrate 80% (10 mL) in ethanol (10 mL) was added dropwise over a 1 h period through the dropping funnel, while keeping the temperature at about 50 °C. The reaction mixture was then refluxed for 1 h and filtered while hot. The solvent was evaporated under reduced pressure to give light yellow precipitate, which was recrystallized from ethanol and dried under vacuum. The yield was 93% (4.0 g); mp 202–204 °C (dec.). FT-IR (KBr): 3335 (m), 3294 (m), 3072 (m), 1691 (s), 1687 (s), 1625 (m), 1643 (m), 1525 (s), 1414 (m), 1322 (s), 1209 (s), 1190 (m), 1152 (m) cm^{-1}.^{1}H NMR (500 MHz, DMSO-d_6), δ (ppm): 3.65 (dd, $J_1 = 13.19$, $J_2 = 7.63$, 2H), 4.90 (dd, $J_1 = 8.22$, $J_2 = 7.02$, 1H), 5.46 (NH_2, 4H), 6.03 (Ar, 1H), 6.62 (Ar, 2H), 7.02–7.17 (Ar, 3H), 7.31 (Ar, 2H), 7.41–7.66 (Ar, 5H), 8.78 (N–H, 1H), 9.57. ^{13}C NMR (125 MHz, DMSO-d_6), δ (ppm): 37.26 (CH_2), 53.16 (CH), 102.11 (Ar), 104.73 (Ar), 122.44 (Ar), 126.40 (Ar), 128.08 (Ar), 128.53 (Ar), 129.77 (Ar), 129.75 (Ar), 136.25 (Ar), 137.26 (Ar), 139.12 (Ar), 148.85 (Ar), 167.15 (C=O), 172.80 (C=O) ppm. Elemental analysis calculated for $C_{21}H_{21}N_4O_2$ (374.44 g mol^{-1}): C, 70.57%, H, 5.92%, N, 14.96%. Found: C, 70.13%; H, 6.09%; N, 14.62%.

Fabrication of NCs

Absolutely dried PMDA was added to a DMF solution of diamine **5** (with the same molar ratios) in several portions and stirred for 1 h at 0 °C. The temperature was raised up to 25 °C and stirred for 2 h to form corresponding poly(amic acid) (PAA) solution. According to the desired titania percentages (assuming the complete conversion of titanate precursor to titania particles) the required quantities of $Ti(OEt)_4$ (dissolved in acac with a molar ratios of 1:4) were added and continuously stirred for 15 h. Thin films of pure PAA and mixed PAA with different percentages of titanate precursor were fabricated by casting onto dust-free glass plates. Resulted thin films were annealed using an electric air-circulating oven at 50, 100, 150, 200, and 250 °C for 1 h each and 300 °C for 10 h and then were cooled and removed from glass surface using a sharp edge blade. The titania percentages were 5, 10, and 15 wt%, which are abbreviated as PIT5, PIT10, and PIT15, respectively.

Results and discussion

Characterization of diamine monomer

A diamine monomer containing L-phenylalanine moiety in the pendant group (**5**) was synthesized according to the synthesis pathway shown in Scheme 1. The FT–IR

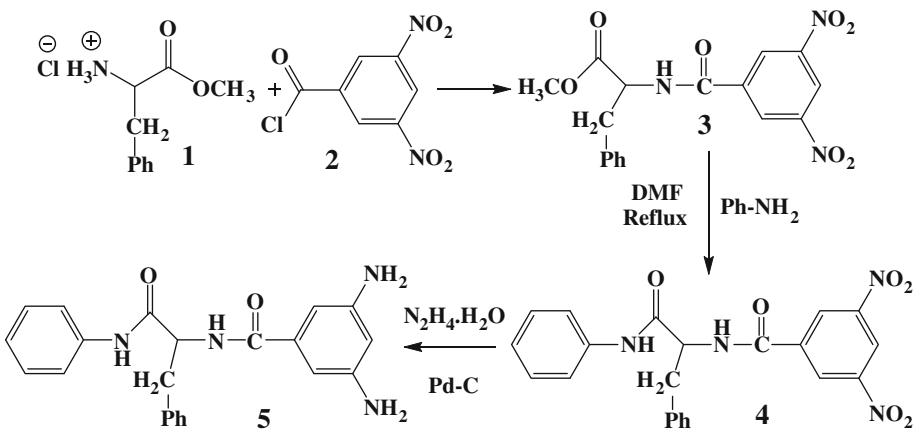

Scheme 1 Synthesis of diamine monomer **5**, containing L-phenylalanine fraction in the pendant group

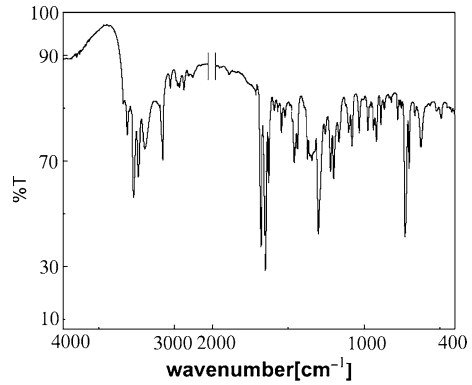

Fig. 1 FT–IR spectrum of diamine monomer **5**

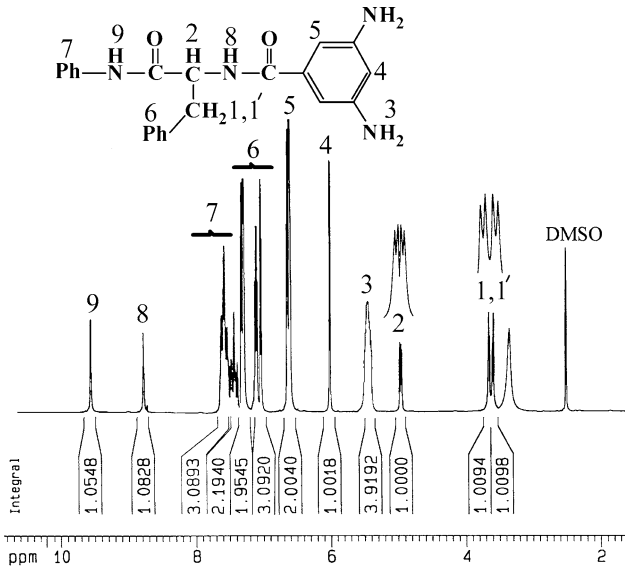

Fig. 2 ^{1}H-NMR spectrum of diamine monomer **5**

absorptions related to the amide carbonyl groups are appeared at 1691 and 1687 cm^{-1} (Fig. 1). The familiar double absorption peaks of amine functions and the amide N–H are obvious around 3250–3350 cm^{-1}. The ^{1}H-NMR spectrum (Fig. 2) confirms the proposed structure for diamine **5**. Two classic doublet of doublet peaks resonated at 3.65 and 4.90 ppm are related to the CH_2 fraction and CH (chiral center), respectively. Both the number and the situation of peaks in ^{13}C-NMR spectra prove the presented chemical structure of diamine **5** clearly (Fig. 3). There was fine agreement between calculated and found amounts of elemental analysis.

Fabrication of nano hybrid films

The room temperature polymerization of diamine **5** and PMDA produced PAA as the premature NC matrix (Scheme 2). Several thin films composed of PAA and $Ti(OEt)_4$ were acquired with different concentrations.

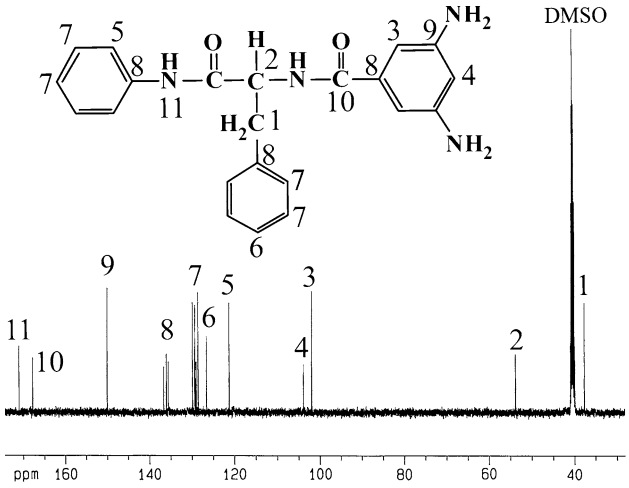

Fig. 3 ^{13}C-NMR spectrum of diamine monomer **5**

In the next step, the annealing of thin films converted the amic acid moieties in the structure of PAA to imide functional groups. Generated water as the imidization byproduct hydrolyzed the titanate precursor to titania particles via a sol–gel process.

Characterization of nano hybrid films

The cyclization of amic acid moieties to imide functions was detected via the FT–IR spectroscopy as well as TGA techniques. There is an extremely broad peak at 2400–3600 cm^{-1} in the FT–IR spectra of PAA related to the carboxylic acid fractions, which is omitted in the other entries showing the complete imidization of amic acid functions (Fig. 4). Furthermore, the vibration peak at 1620 cm^{-1} of PAA is failed in the spectra of annealed films which confirm the complete cyclization once more. The other evidences for the full imidization are the absorption peaks at 1720 and 1376 cm^{-1} related to the stretching of imide C=O and C–N bonds, respectively.

In the spectra of PIT5–PIT15, the absorption peaks at 400–750 cm^{-1}, corresponding to Ti–O bonds, become more intensive with the increase in titania contents. The UV–Vis spectra of nano hybrid films (Fig. 5) show the decrease in *T%* as a result of increase in the titania contents. The potential reasons for this behavior are the more agglomeration of titania nanoparticles and/or the formation of titanium ion-acac complex. However, the later one could be negligible after the gelation process [36].

Morphology

The morphology of nano-sized titania was investigated using both TEM photographs and XRD patterns of NCs. According to the TEM photographs (Fig. 6), the fabricated NCs not only are well-dispersed in the polymer matrixes

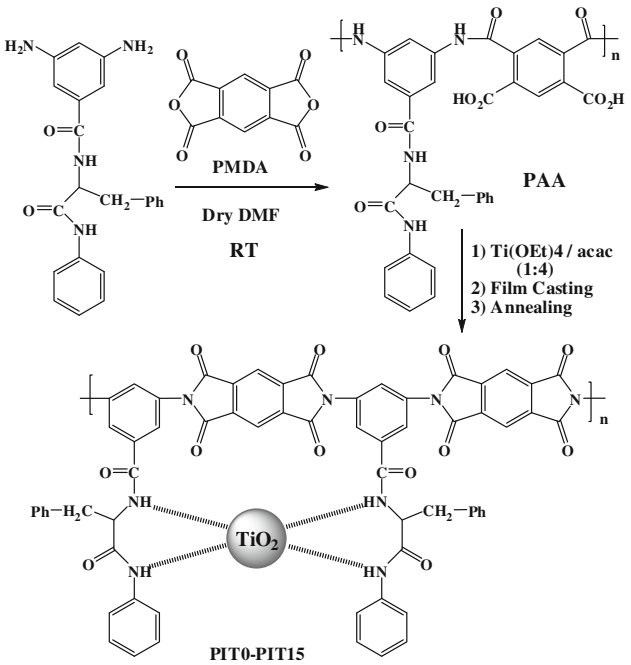

Scheme 2 Fabrication pathway for PI/titania nano hybrid films

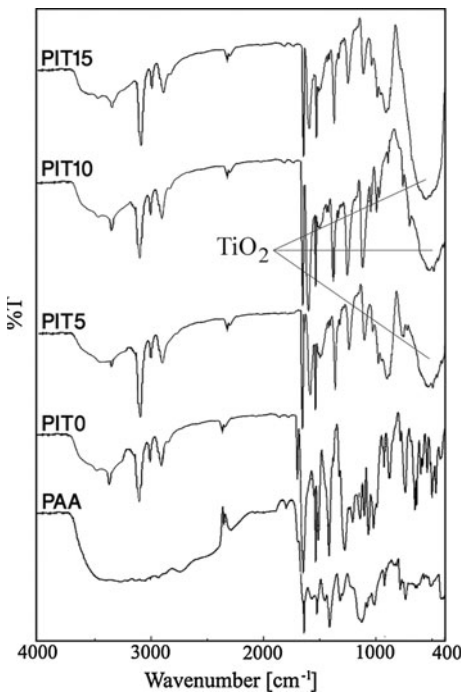

Fig. 4 FT–IR spectra of PAA and PIT0–PIT15

but also have spherical shape which is preferred due to the highest surface area to volume ratio. This observation possibly is due to the intensive surrounding of titania particles by polymer matrix via the construction of strong polymer–inorganic interactions. The interactions of amide N–H (H-bonds) and/or oxygen's nonbonding electrons,

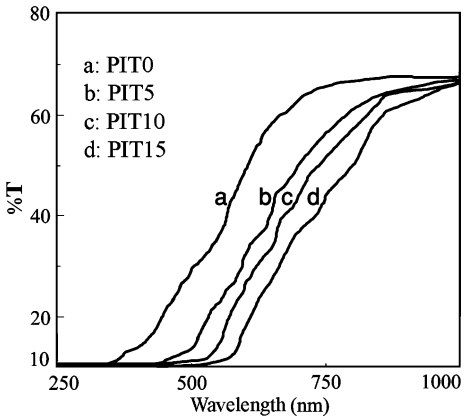

Fig. 5 UV–Vis spectra of PIT0–PIT15

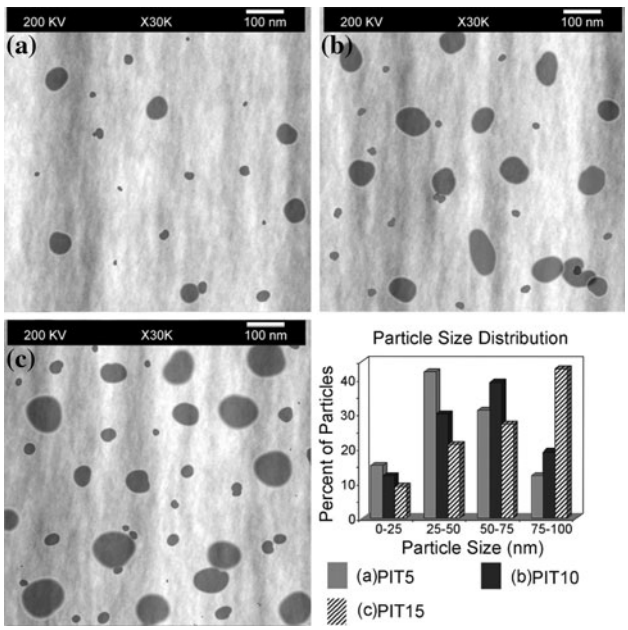

Fig. 6 TEM photographs of PIT5–PIT15 and their size distribution diagram

existed in the polymer matrix- and titania nanoparticles, have played significant role in the regulations of particles distributions as well as shapes. It has been shown that not only the H-bond interactions between NH and Ti–OH groups but also the self H-bond involving the amide C=O and NH will cause an absorption peak at 3200–3600 cm^{-1} [37]. Thus, in this study the differences between the FT–IR spectra of pure PI matrix and that of NC films are not superficial (Fig. 4). The formation of relatively strong organic–inorganic interactions is more apparent via the comparison of glass transition temperatures (T_g) of fabricated materials discussed in the "Thermal properties" section. Moreover, the existence of bulky pendant groups in the structure of PI improved the interactions of polymer

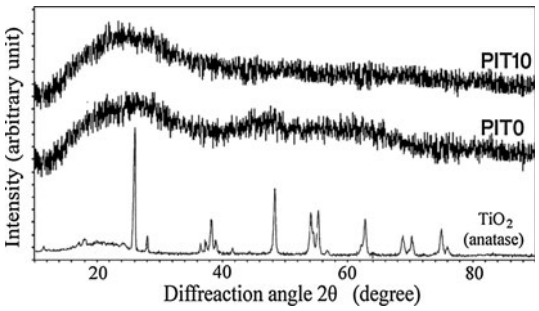

Fig. 7 XRD patterns of pure anatase titania, PIT0, and PIT10 as a typical NC

matrix with titania nanoparticles via the increasing of free volume and thus, the facilitating of segmental movements.

In comparison with the previous study, in this study, probably the more flexible polymer chains have caused the more efficient organic/inorganic interactions and thus the better distribution of nanoparticles as well as more spherical shapes. The size distribution diagram shows that in the NCs with the lower titania percentages, there is the more tendency to form the smaller particle sizes and vise versa. This behavior may be attributed to the both faster gelation step and more agglomeration of nanoparticles at the higher titania contents.

The XRD spectra of anatase titania, pure polymer matrix, and one representative NC are illustrated in Fig. 7. Predictably, the presented sample (PIT10) does not show crystalline pattern. The others NCs showed comparatively the same patterns. The creation of amorphous titania through the described sol–gel procedure is a familiar observation [35, 37].

Thermal properties

Figure 8 shows the TGA thermograms of fabricated NC films with various titania contents. Obviously, the more titania percentages have led to the more char yields at 800 °C confirming the superior heat resistance. Although,

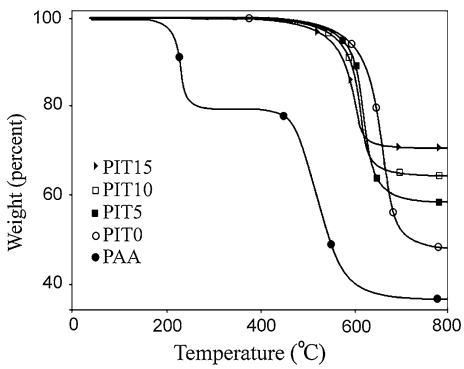

Fig. 8 TGA thermograms of PAA and PIT0–PIT15 under N_2 atmosphere at a heating rate of 20 °C min^{-1}

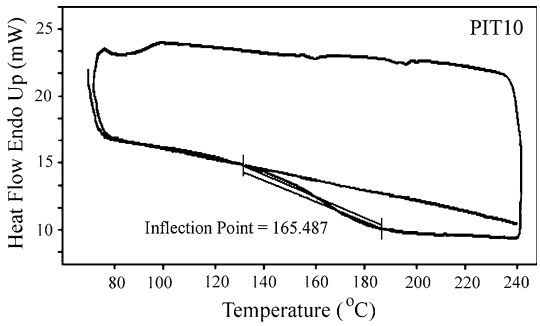

Fig. 9 DSC thermogram PIT10 under N_2 atmosphere at a heating rate of 20 °C min^{-1}

Table 1 The T_g values measured using DSC analyses

Entry	Material	Titania contents (wt%)		T_g (°C)[c]
		Theory[a]	Experiment[b]	
1	PIT0	0	0	142.9
2	PIT5	5	4.67	153.1
3	PIT10	10	9.52	165.5
4	PIT15	15	14.12	172.6

[a] The theoretical TiO_2 content was calculated under the assumption that the sol–gel reaction proceeds completely

[b] The experimental TiO_2 content was obtained from residual ash after heat treatment at 900 °C by TGA

[c] Measured at a heating rate of 20 °C min^{-1} under N_2 atmosphere

an insignificant decrease in the weight percents occurs at the lower temperatures which is related to the familiar oxidative decomposition catalyzed by metal oxide component [36–38]. In order to verify the precise temperatures of the initiation and the completion of imidization process, the PAA was tested by TGA too and they found to be at 180 and 290 °C, respectively. The lack of this weight loss in the thermograms of PIT0–PIT15 proves their complete imidization through gradual annealing.

The DSC analysis was used to verify the T_gs of fabricated materials. One representative DSC thermogram is presented in Fig. 9. The other materials showed more or less the same patterns.

A comparison of the determined T_g values (Table 1) with literatures shows that they are considerably smaller than related hybrid materials [20]. It may be attributed to the existence of bulky pendant groups in the structure of polyimide matrix which make the polymer backbone more flexible. The other suspected reason may be the lower molecular weight of polymers. Obtained data showed the enhancement in T_g values with the increase in titania contents confirming the improvement in the thermal stability as a results of the incorporation of nano-inorganic particles. Besides, this phenomenon could be the other

evidence for the operating of burly organic–inorganic interaction.

Conclusions

In this study, two multi-purpose materials (PI and titania) are the fundamental constituents for fabrication of new series of functional NC thin films. PI matrix has provided a powerful media, for generation of titania nanoparticles via a sol–gel manner, beside its effective role in the distribution of titania nanoparticles. On the other hand, titania nanoparticles have increased the thermal stability of resulted materials as well as the improvement in UV–Vis blocking efficiency. The synthesis and full characterization of a new L-phenylalanine containing diamine are presented. Fabricated diamine was applied for the in situ sol–gel fabrication of a series of PI/titania nano hybrid thin films. As TEM photographs confirmed, the titania particles sizes were below 80 nm, well-dispersed in the PI matrix, and also enjoys the favorable spherical shapes which are attributed to the relatively strong polymer–inorganic interactions. Furthermore, the incorporation of bulky pendant groups in the structure of PI matrix increased segmental movements of polymer chains and thus not only facilitated the surrounding of nanoparticles by polymer ground, which led to the improved particles distributions and shapes, but also enhanced their processability. According to the XRD patterns, titania nanoparticles possess the expected amorphous structures. The thermal analysis (TGA and DSC) of fabricated NCs showed the elevated heat resistance by increase in titania contents. NCs with the higher titania contents absorbed the UV–Vis more efficiently. The prospective bioactivity of the fabricated amino acid containing nano hybrid materials may be the subject of further investigations.

Acknowledgements Financial support for this study from Research Affairs Division Islamic Azad University, Kazerun Branch, Iran, and Iran nanotechnology Initiative Council and National Elite Foundation (NEF) is greatly acknowledged.

References

1. Chau JLH, Liu HW, Su WF (2009) J Phys Chem Solid 70:1385
2. Karim MR, Lim KT, Lee MS, Kim K, Yeum JH (2009) Synth Met 159:209
3. Xu L, Xia Yang, Guo Y, Ma F, Guo Y, Yuan X, Huo M (2010) J Hazard Mater 178:1070
4. Mi O, Ru B, Yi X, Cheng Z, Chune-an M, Mag W, Hong-zheng C (2009) Trans Nonferrous Met Soc China 19:1572
5. Shah J, Yuan Q, Misra RDK (2009) Mat Sci Eng A 523:199
6. Xie Y, Huang C, Zhou L, Liu Y, Huang H (2009) Compos Sci Technol 69:2108
7. Ngo VG, Bressy C, Leroux C, Margaillan A (2009) Polymer 50:3095
8. Sun L, Gibson RF, Gordaninejad F, Suhr J (2009) Compos Sci Technol 69:2392
9. Takahashi S, Paul DR (2006) Polymer 47:7519
10. Gutierrez-Tauste D, Domenech X, Casan-Pastor N, Ayllon JA (2007) J Photochem Photobiol A 187:45
11. Amjadi M, Rowshanzamir S, Peighambardoust SJ, Hosseini MG, Eikani MH (2010) Int J Hydrogen Energy 35:9252
12. Skorb EV, Ustinovich EA, Kulak AI, Sviridov DV (2008) J Photochem Photobiol A 193:97
13. Li J, Yang X, Yu X, Xu L, Kang W, Yan W, Gao H, Liu Z, Guo Y (2009) Appl Surf Sci 255:3731
14. Bellachioma G, Ciancaleoni G, Zuccaccia C, Zuccaccia D, Macchioni A (2008) Coord Chem Rev 252:2224
15. Mandzy N, Grulke E, Druffel T (2005) Powder Technol 160:121
16. Hojati B, Sui R, Charpentier PA (2007) Polymer 48:5850
17. Hu Q, Marand E (1999) Polymer 40:4833
18. Lee CH, Tenhaeff W, Gleason KK (2009) Thin Solid Films 517:3619
19. Huang SH, Chen DH (2009) J Hazard Mater 163:174
20. Tsai MH, Whang WT (2001) Polymer 42:4197
21. Yudin VE, Otaigbe JU, Gladchenko S, Olson BG, Nazarenko S, Korytkova EN, Gusarov VV (2007) Polymer 48:1306
22. Wang H, Zhong W, Xu P, Du Q (2005) Composites A 36:909
23. Kim YJ, Chung IS, In I, Kim SY (2005) Polymer 46:3992
24. Spiliopoulos IK, Mikroyannidis JA (1998) Macromolecules 31:515
25. Yang CP, Su YY, Hsu MY (2006) Colloid Polym Sci 284:990
26. Murugan R, Ramakrishna S (2004) Biomaterials 25:3829
27. Chow D, Nunalee ML, Lim DW, Simnick AJ, Chilkoti A (2008) Mat Sci Eng R 62:125
28. Angiolini L, Benelli T, Giorgini L, Mauriello F, Salatelli E, Bozio R, Dauru A, Pedron D (2007) Eur Polym J 43:3550
29. Katsarava R (2003) Macromol Symp 199:419
30. Art-Haddou H, Leeder SM, Gagne MR (2004) Inorg Chim Acta 357:3854
31. Sanda F, Endo T (1999) Macromol Chem Phys 200:2651
32. Zhao R, Torley P, Halley PJ (2008) J Mater Sci 43:3058. doi: 10.1007/s10853-007-2434-8
33. Kumar P, Sandeep KP, Alavi S, Truong VD, Gorga RE (2010) J Food Eng 100:480
34. Broedling NC, Hartmaier A, Buehler MJ, Gao H (2008) J Mech Phys Solids 56:1086
35. Seyedjamali H, Pirisedigh A (2011) Colloid Polym Sci 289:15–20
36. Liaw WC, Chen KP (2007) Eur Polym J 43:2265
37. Tsai MH, Chang CJ, Chen PJ, Ko CJ (2008) Thin Solid Films 516:5654–5658
38. Chiang PC, Whang WT (2003) Polymer 44:2249